IIETA International Information and Engineering Technology Association
Advancing the World of Information and Engineering

Mathematical Modelling of Engineering Problems
Vol. 12, No. 5, May, 2025, pp. 1615-1626
Journal homepage: http://iieta.org/journals/mmep

# Design and Evaluation of a Parallel Manipulator for Interconnected Transmission Tracking

Kaushik Patel[1*], Pravin Patel[2], Chandrakant Sonawane[3,4], Arun Kumar Bongale[3], Ghanshyam G. Tejani[5,6], Subhav Singh[7,8,9], Deekshant Varshney[10,11], Choon Kit Chan[12]

[1] Department of Mechanical Engineering, Government Engineering College Patan, Gujarat 384265, India
[2] Department of Electrical Engineering, Government Engineering College Patan, Gujarat 384265, India
[3] Symbiosis Institute of Technology (SIT), Symbiosis International Deemed University (SIU), Pune 412115, India
[4] Symbiosis Centre for Nanoscience and Nanotechnology, Symbiosis International Deemed University (SIU), Pune 412115, India
[5] Department of Research Analytics, Saveetha Dental College and Hospitals, Saveetha Institute of Medical and Technical Sciences, Saveetha University, Chennai 600077, India
[6] Applied Science Research Center, Applied Science Private University, Amman 11931, Jordan
[7] Chitkara Centre for Research and Development, Chitkara University, Himachal Pradesh 174103, India
[8] Division of Research and Development, Lovely Professional University, Punjab 144411, India
[9] Centre for Promotion of Research, Graphic Era (Deemed to be University), Uttarakhand, Dehradun 248002, India
[10] Centre of Research Impact and Outcome, Chitkara University, Punjab 140417, India
[11] Division of Research & Innovation, Uttaranchal University, Dehradun 248007, India
[12] Faculty of Engineering and Quantity Surveying, INTI International University, Nilai, Negeri Sembilan 71800, Malaysia

Corresponding Author Email: Kaushik.patel@gecpatan.ac.in



https://doi.org/10.18280/mmep.120516

**Received:** 5 December 2024
**Revised:** 2 April 2025
**Accepted:** 15 April 2025
**Available online:** 31 May 2025

***Keywords:***
*parallel robotics, kinematic analysis, dynamic simulation, process innovation*

**ABSTRACT**

This study presents the design, modeling, fabrication, and experimental validation of a two-degree-of-freedom (2-DOF) robot integrated with a novel Revolute-Spherical-Spherical-Revolute-Spherical-Spherical (RSSR-SS) parallel tracking mechanism for manufacturing and space-oriented applications. Each joint is independently actuated by a DC motor with gear reduction and angular position sensors. Mechanical components were designed using SolidWorks and fabricated following a detailed production workflow. Kinematic and dynamic analyses were conducted using MATLAB and verified through simulation with the Robotics Toolbox. The inverse kinematics problem was resolved using a geometric approach. Experimental tests demonstrated high positioning precision and repeatability of the end-effector. The RSSR-SS mechanism—featuring three extendable rods with spherical joints or compound linkages—offers superior rigidity, minimal inertia, and enhanced tracking accuracy compared to traditional serial mechanisms. These results confirm the system's potential for deployment in precision-driven environments, such as solar tracking or space communications, where reliability and efficiency are critical.

## 1. INTRODUCTION

The joint connections found within the RSSR-SS platform are characterized by bound interactions, which provide the joint flexibility often seen in Rotary and Universal joints. This flexibility enables the plate to move in a manner that accommodates its specific requirements. The text delineates the procedural aspects including the fabrication of diverse components, assembly of the model, and establishment of the experimental framework. Multiple techniques are used in the manufacturing process of each unique item. The SolidWorks software is used to create models of various components of the RSSR-SS platform and assemble the final product. The modal analysis further demonstrated the dynamic behaviour of the spring. The determination of the optimal Universal joint profile for the RSSR-SS platform involves the construction of an assembly and complete model using the Solid Works application, using specific assembly processes. The Solid Works software has many connections to facilitate the visualization of the top plate's functionality. In order to provide an appropriate range of motion for the plate on the RSSR-SS platform, all joint connections are established using bonded connections and universal joints. Every component is meticulously crafted using a variety of techniques.

Minimizing the dimensions, physical volume, and financial expenditure associated with the extendable road tracker's pivotal elements constitutes a critical undertaking in the realm of design. In general. Any application needs at the very least a database in the form of a large array that is used in the transmission antenna [1, 2]. Large apertures allow the tracker with combined array, achieving the primary goals of decreasing the tracker's bulk, storage capacity, cost etc. It also

deployed surface area without compromising on performance too. The integration of Jacobian Matrix in single planar device called a Flat Plate Structure (FPS) is now the primary topic of research work [3]. A concentrator in the shape of a Flat receiver mounted on RSSR-SS plat, it outperforms the FPS in terms of conversion efficiency while having a lower surface density [4]. Space applications have utilised large-aperture receiver antennas and concentrators. The receiver surface, like the solar disc concentrator, reflects electromagnetic waves and sunlight [5]. On the other hand, the combination of these two technologies has only been the subject of a limited number of research paper published by researchers. The parabolic reflector antenna developed by Sukri et al. [6] presented a novel approach for improving robotic arm precision through numerical code recognition, enabling efficient and automated object handling in industrial and manufacturing applications. Singh et al. [7] described a design for a power antenna that makes use of a paraboloid reflector made from an inflated membrane. Rigid structure of the platform is composed of a two RS Dyads and one SS Dyad [8], which are interconnected by flexible wires. This surface serves as a substrate for the deposition of aluminized membrane facets.

The manipulator can focus both electromagnetic radiation and sunlight. The tracker plate is attached to the central cylinder at the focal plane of the Consortium for Marine Robotics (CMR), allowing for the switching between collecting electromagnetic radiation and capturing solar rays [9].

The coordinate system spirals when a tracker is in a Sun-Synchronous Equatorial Orbit (SSEO). This spiral path can be approximated as a circular track for one orbit [10]. The Solar Power Photovoltaic Conversion Interface lies in the middle of the tracker's orbital plane and sun-facing plane due to solar wings and the sun's location relative to the earth [11]. Besides the above parameters, the tracker must meet the following. The requirements for a solar panel tracking system in space can be summarized as follows: (1) the system should possess an ample workspace that enables a broad range of motion, facilitating the tracking of the sun and orientation towards the ground station; (2) the structure of the system should be uncomplicated yet dependable, catering to the specific demands of space missions; and (3) the system should exhibit a high level of precision in pointing, ensuring efficient power generation or communication capabilities [12].

In space applications, the most prevalent multifaceted rotation tracking systems, known as RSSR-SS, employ a serial mechanism featuring azimuth and elevation components [13]. Parallel mechanisms provide benefits over serial mechanisms, including a simple and lightweight design, better structural rigidity, decreased inertia, increased dependability [14], and superior platform positioning and pointing [15, 16]. Despite various parallel techniques with two-dimensional rotation, few have been implemented in space applications. This study introduces a rotating parallel mechanism that has two degrees of freedom (2-DOF) and incorporates a redundant drive system, specifically designed for the purpose of antenna targeting [17, 18]. The use of a parallel mechanism with redundancy has the potential to enhance both the precision of targeting and the capacity and reliability of the payload, as compared to a non-redundant counterpart. The redundancy drive is used to improve system efficiency, but this comes at the cost of increased system size, volume, cost, and energy consumption. Inefficient use of linear drive results in wasteful energy usage, even after the extra drive rod has been eliminated. Accordingly, the RSSR SS would benefit from a different methodology.

With the goal of regulating the position of RSSR SS tracking parallel manipulator, a three-degree-of-freedom (3-DOF) parallel pointing system has been created. The construction of this mechanism has resemblance to the ones described in references [19, 20]. However, its limb chain is made up of four rotary joints and tow spherical joint in extendable connecting rods. The system is thus not as stiff or accurate in its tracking as it could be. It's important to mention that each branch in the chain consists of five rotary joints, and this configuration has been observed to decrease the reliability of the mechanism [21]. It can be proved mathematically that this approach is inappropriate for implementation in the RSSR SS since the number of unknowns exceeds the number of equations. A compliant 2-degree-of-freedom (DOF) pointing mechanism for spacecraft thrusters, antennas, and Jacobian array systems was proposed by Li and Wang [22]. However, it's important to note that the rotation range of this pointing mechanism is limited to just 15°, which does not meet the wide-ranging rotation requirements specified for RSSR SS. RSSR-SS parallel mechanisms with more than three degrees of freedom have found applications in various areas, including pointing for space remote sensors, active vibration isolation for precise space payloads, and the end effector of space station transposition mechanisms. However, it's crucial to emphasize that RSSR SS only necessitates rotation in two dimensions, rendering none of the aforementioned options suitable for use as the RSSR SS tracker. To fulfill the requirements of the RSSR SS tracker, there's a need to develop a TER parallel tracker, specifically the 3-RPS parallel manipulator [23-25]. This choice has the potential to enable the RSSR SS to accurately track the sun or reposition itself toward the ground station, addressing the limitations mentioned earlier. The 3-RPS mechanism is characterized by its simplicity and lightweight nature, offering structural stability, durability, and improved positioning and orientation capabilities for the mobile platform when compared to sequential mechanisms. The linear extendable rods in the TER tracker contribute to energy efficiency and eliminate the need for bulky speed reducers, which are typically required for monitoring the relatively modest movement speed of RSSR SS. However, it's worth noting that there is limited literature available on 3-RPS parallel manipulators in the context of spaceship appendages. This study aims to examine, formulate, and empirically verify the RSSR SS model of the TER tracker, as detailed in the following section. The kinematic model is converted to a dynamic model using the Newton-Euler formulation [26]. The TER tracker's motion trajectory is specifically designed either for sun tracking or reorientation toward the ground station, as outlined in reference [27]. In the upcoming section, this research configures parameters to assess the TER tracker's workspace and pointing accuracy and conducts simulations to evaluate its performance. Additionally, MATLAB is used to calculate the TER tracker's drive power. Initial ground-based testing for sun monitoring with the TER tracker has yielded positive results. The subsequent section will delve into the findings of this work.

This work introduces an innovative Three-Extendable-Rod (TER) tracker incorporated into a 3-RPS parallel manipulator for the RSSR-SS platform, intended for dual-purpose space applications related to solar energy harvesting and terrestrial communication. This design provides a lightweight, compact, and energy-efficient alternative to conventional serial or bulky

redundant mechanisms, with improved pointing precision and structural rigidity.

## 2. RSSR-SS EXTENSIBLE-ROD TRACKER

Figure 1 and Figure 2 display the complete representation of the RSSR-SS, along by its corresponding description. The connection between the RSSR-SS and the Platform is established using a rod that has a rotating joint at its lower end, housing a motor for deployment purposes. At its upper end, the rod is affixed to the platform on which the Spherical tracker is situated, utilizing a stationary joint [28]. The tracker's movable platform is attached to the central cylinder's bottom by a rotary joint with a motor that deploys the PLC Control. Figure 2 shows how three adjustable-length rods allow a mobile platform to revolve around the body coordinate system's Yb axis. As depicted in Figure 2, when the RSSR-SS system requires reorientation towards the ground station for communication purposes, the Platform with Tracker component maintains a consistent elevation angle by tracking the movement of the sun and rotating along the Yb axis towards the Zb axis. At the same time, the second Dyad part revolves around the rotary joint at the central cylinder's base until the axis of the cylinder is perpendicular to the equator [29].

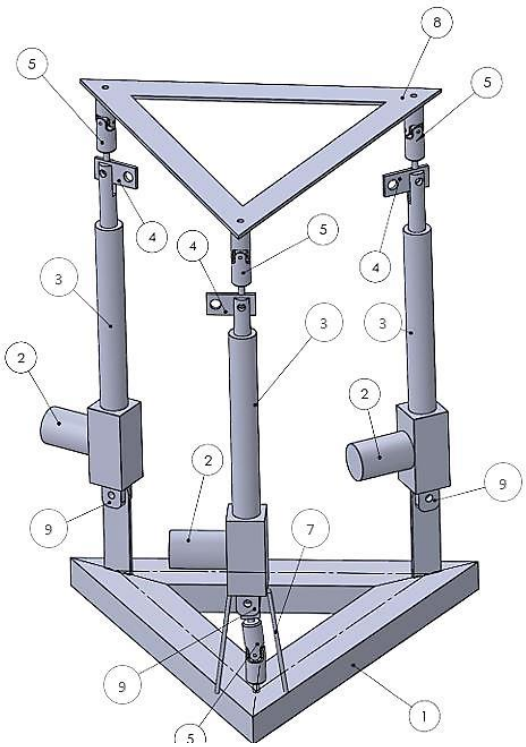

**Figure 1.** RSSR-SS linkage

All mechanical component 3D design and assembly made full use of SolidWorks CAD tools. The comprehensive simulation features and exact tolerance modeling of this platform were reasons it was chosen. The manipulator's each leg was designed with a closed-loop kinematic chain using rotary joints at the base and spherical joints at the top ends. Derived from the 3-RPS parallel mechanism structure, which is typified by three revolute-prismatic-spherical limbs, kinematic equations for forward and inverse solutions were derived. Because of their computational simplicity and efficiency in real-time execution, geometric approaches resolved the inverse kinematics. Closed-form Jacobian matrix mapping of the kinematic constraints allowed one to examine the velocity and orientation of the platform. The kinematic and dynamic models of the RSSR-SS Tracker were replicated using MATLAB and Peter Corke's Robotics Toolkit. Under several sun-tracking and ground-station-pointing conditions, simulations evaluated workspace volume, joint velocity profiles, and actuator force needs.

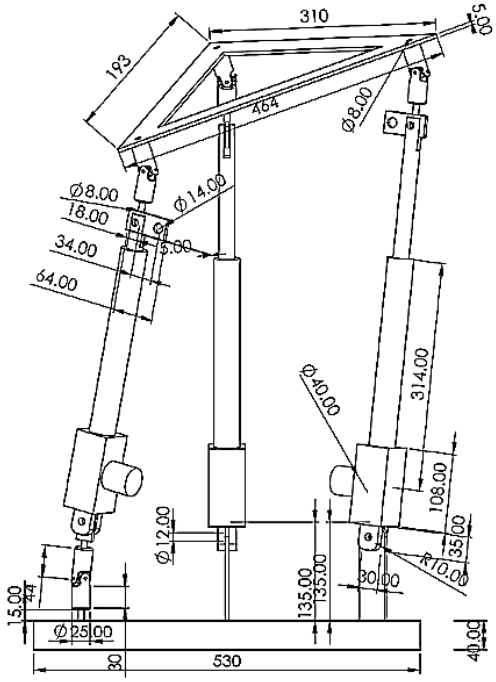


**Figure 2.** RSSR-SS linkage with dimension

### 2.1 Description of RSSR-SS extensible-rod tracker

Figure 3 shows the lightweight and compact construction of the tracker for the RSSR-SS platform. A stationary base platform, a movable base platform, and three extendable rods make up the RSSR-SS platform tracker. Both the stationary and mobile platforms are in the form of wheels, making them far lighter than their solid counterparts. The three rods may be stretched to any desired length inside the space between the two floors, forming a triangle configuration. The connection between each flexible rod and the bottom platform is established by a rotary joint, while the top platform is connected to the rods through a Spherical joint. These joints create a smart compound joint, where the axes of the spherical joint converge at a single point. The RSSR-SS platform tracker offers more flexibility due to the use of a smart compound joint, which also simplifies the manufacturing process compared to a spherical joint. Previous research [28] has shown that the tracker used in the RSSR-SS platform has a total of two degrees of freedom. Specifically, it is capable of rotation along two distinct axes and vertical movement autonomously. The RSSR-SS multiloop parallel manipulator needs a minimum number of two revolutions in order to achieve completion. The rocket fairing has the capacity to accommodate a smaller RSSR-SS platform tracker, provided that the mobile platform is retracted towards the base platform by translational motion. The tracker implemented on the RSSR-SS platform exhibits a low level of inertia, a rapid

response time, and a notable degree of tracking precision, all while maintaining a lightweight and simple design.

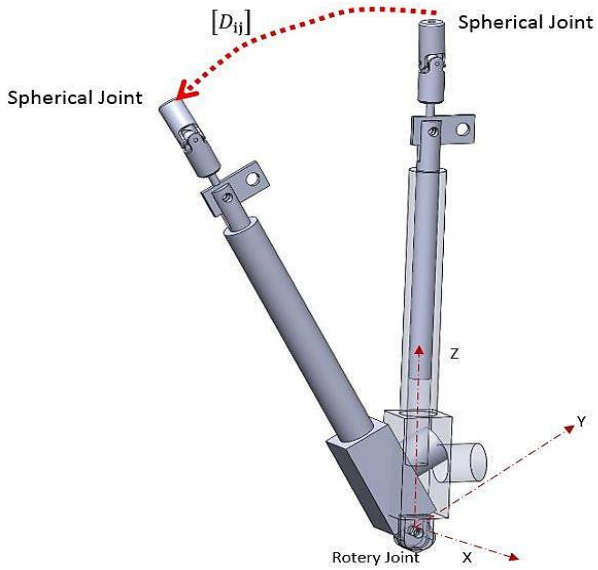


**Figure 3.** Revolute-sphere link

## 3. TRAJECTORY AND MOVEMENT GENERATION OF RSSR-SS MECHANISM

When designing a function-generating mechanism, it's vital to correlate incoming and outgoing connections' rotational movement; this leads to a predictable output from a known input. Connecting a system's input and output. When *x* changes, *y=f(x)* travels over an interval. When input and output are rotated in the same direction, x and y coordinates match. Function generator connection movement. The link connects to and is driven by the Actuator link's movement as shown in Figures 4-6.

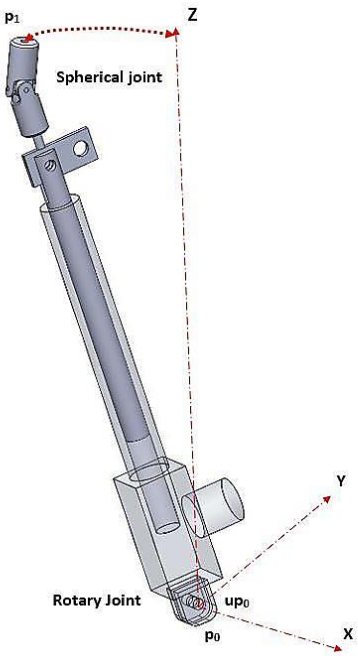


**Figure 4.** R-S link and rigid body points

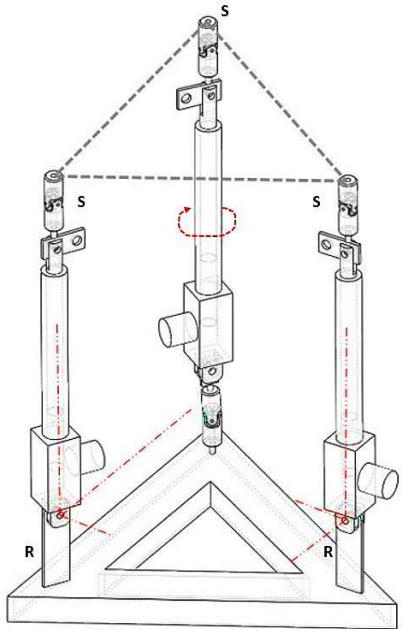


**Figure 5.** RSSR-SS mechanism with passive

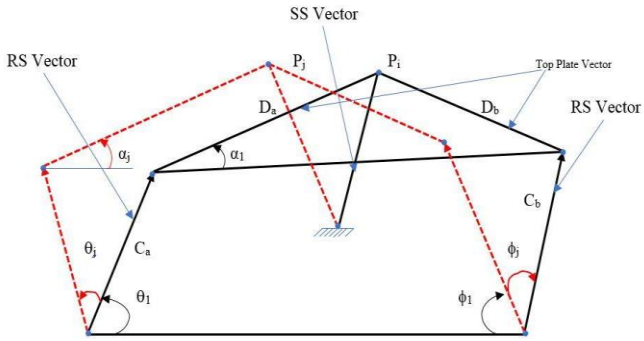


**Figure 6.** Generation of trajectory DOF to ground link

As illustrated, vectors may be used to depict mechanisms' connections. Multiple vector combinations show dimensional synthesis resolutions. One technique uses vector pairs to do dimensional synthesis. Figure 6 shows four-bar relationship is represented by dyads.

Both $C_a$ and $C_b$ originate at the ground pivot and end at the mobile pivot, whereas $D_a$ and $D_b$ originate at the mobile pivot and terminate at the tracer point:

$$C_a e^{(\theta_j + \theta_1)} + D_a e^{(\alpha_j + \alpha_1)} - C_a e^{\theta_1} - D_1 e^{\alpha_1} - P_j + P_1 = 0$$

Following are some design equations that may be derived by using the identity of Euler and distinguishing between the real and imaginary parts of a function:

$$C_a cos(\theta_j + \theta_1) + D_a cos(\alpha_j + \alpha_1) - C_a \cos(\theta_1) - D_a \cos(\alpha_1) - P_{jx} - P_{1x} = 0$$

$$C_a sin(\theta_j + \theta_1) + D_a sin(\alpha_j + \alpha_1) - C_a \sin(\theta_1) - D_a \sin(\alpha_1) - P_{jy} - P_{1y} = 0$$

$C_b$ and $D_b$ are a right dyad of the mechanism, as illustrated in Figure 7. A terrestrial pivot serves as the starting point for the $C_b$, which then returns there at its conclusion. $C_d$ stops at the tracer's endpoint.

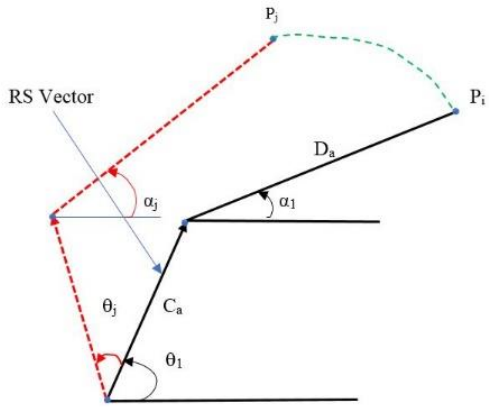


**Figure 7.** Right-hand movement of a RSSR-SS mechanism (RS Dyad)

The corresponding equation for a complete circuit in the correct dyad is

$$C_a e^{(\phi_j + \phi_1)} + D_a e^{(\alpha_j + \alpha_1)} - C_a e^{\phi_1} - D_1 e^{\alpha_1} - P_j + P_1 = 0$$

The real component of the imaginary and the following design equations are derived by considering the left RS dyad and the right RS dyad, respectively:

$$C_a cos\left(\phi_j + \phi_1\right) + D_a cos(\alpha_j + \alpha_1) - C_a \cos(\phi_1) - D_a \cos(\alpha_1) - P_{jx} - P_{1x} = 0$$

$$C_a sin\left(\phi_j + \phi_1\right) + D_a sin(\alpha_j + \alpha_1) - C_a \sin(\phi_1) - D_a \sin(\alpha_1) - P_{jy} - P_{1y} = 0$$

The following equation for a Trajectory may be solved in MATLAB, yielding a very precise position.

## 4. ALGORITHM FOR SYNTHESIS OF RSSR-SS MECHANISM

The following MATLAB code illustrates the concept of following the path and movement of individual precision points in relation to RS and SS dyads (Figure 8). It is common practice for software programs to create test data in the following fashion: Many people think this way.

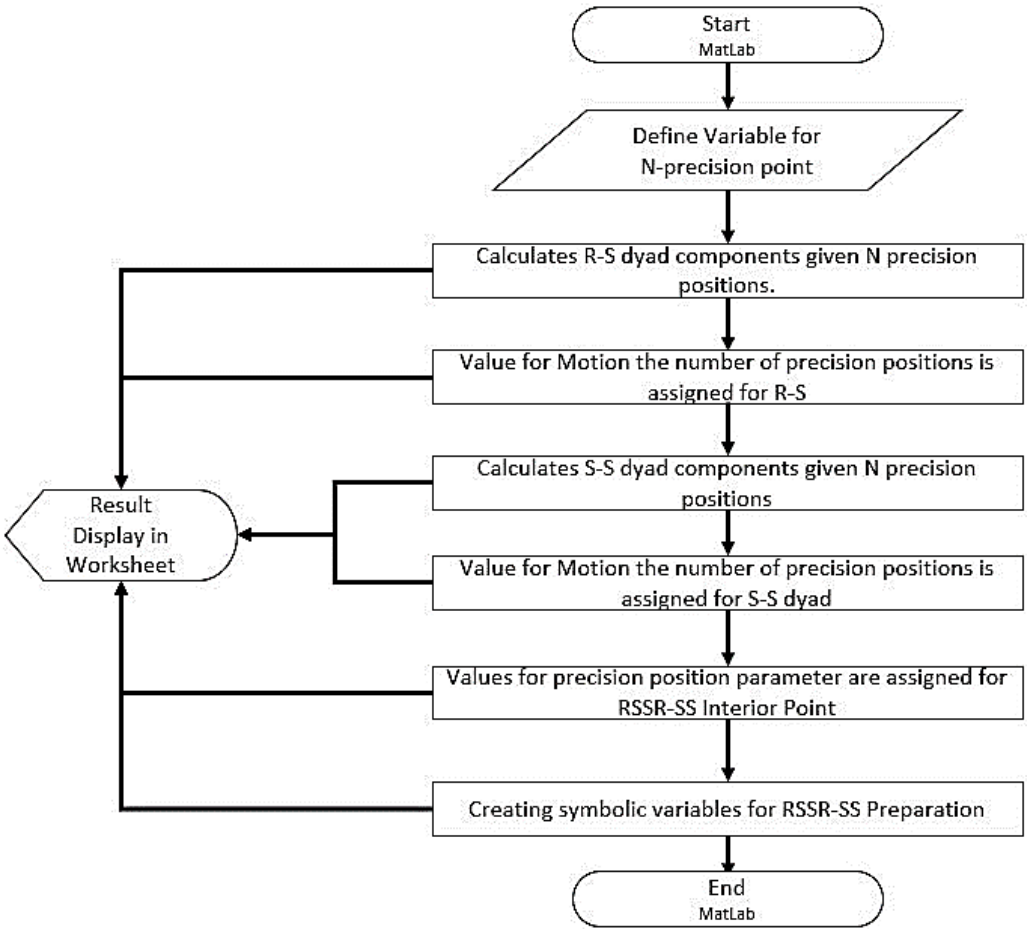


**Figure 8.** Algorithm for synthesis of RSSR-SS mechanism

In order to reach each required point, the equations for both dyads must be solved, at which point the size and angles of the linkages are determined. In order to generate a trajectory, we use the parameters determined from MATLAB for a variety of RSSR-SS rotation angles.

## 5. DIMENSIONAL SYNTHESIS FOR THE MECHANISM WITH KINEMATIC PAIRS RSSR-SS

Kinematic synthesis is constructing a task-capable machine. Kinematic synthesis includes function, trajectory, and movement creation. As stated in Section 3, only the RSSR-SS mechanism will be synthesised here. The mechanism has five

links, one permanent and four movables. RSSR is crucial for function creation and has been examined extensively. RSSR-SS topology must overcome the mechanism's floating link issue. It recommends constructing a trajectory and linking a rigid body.

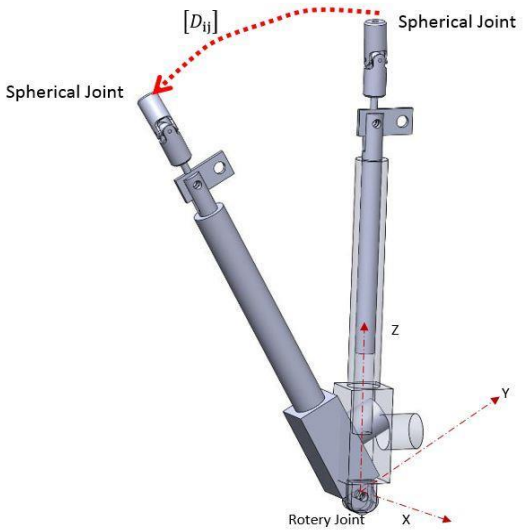


**Figure 9.** Analogy between linear displacement and angle of rotation

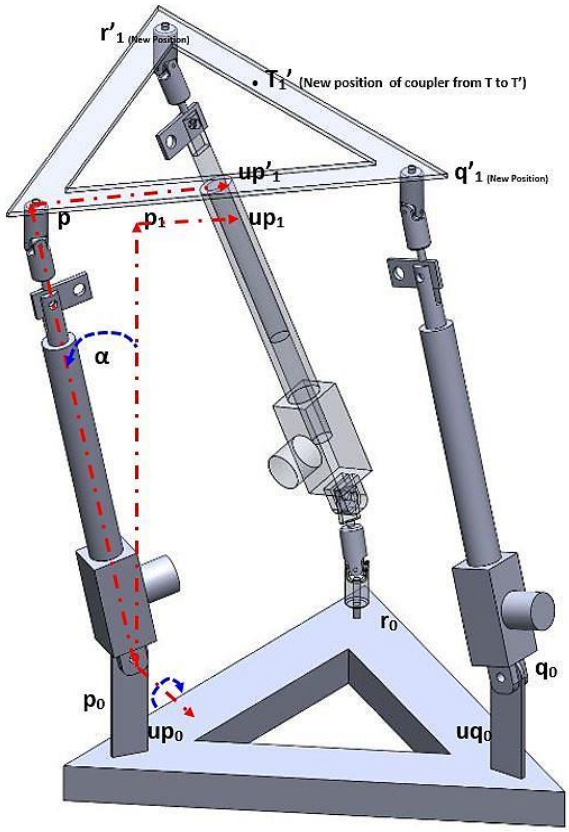


**Figure 10.** RSSR-SS mechanism rotate about angle a-up

Dimensional synthesis is a subset of kinematic synthesis that involves determining the lengths (dimensions) of a mechanism's connections [30]. Figure 9 shows how a random point p travels between 1 and j. It is shown by p1 and pj, which are called precision points to studied mechanism to meet these goals.

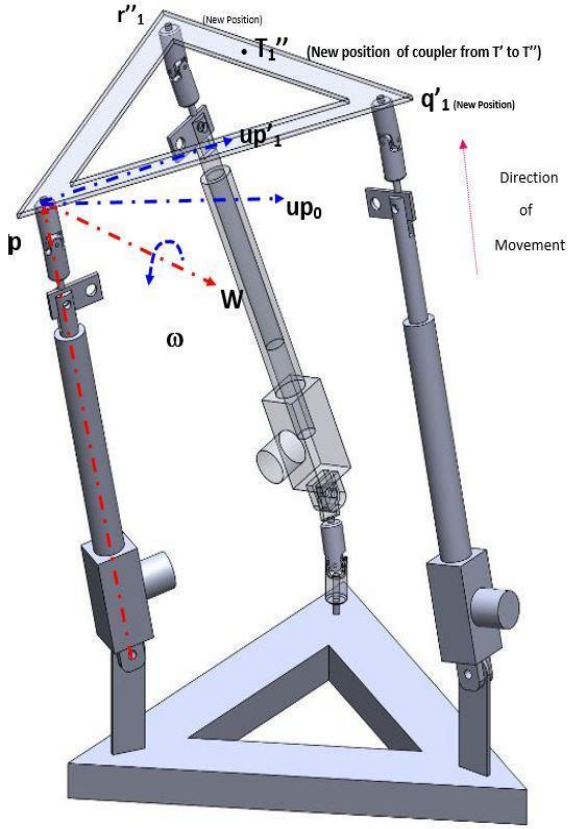


**Figure 11.** RSSR-SS mechanism rotate about angle w

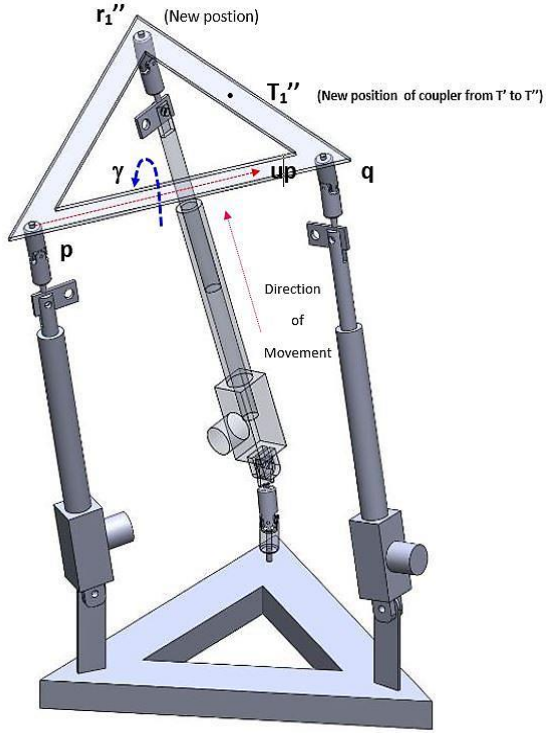


**Figure 12.** RSSR-SS mechanism rotate about angle w rigid body rotation

The composite rotation matrix converts vector coordinates to xyz. It represents the matrix's composite rotation matrix. Multi-loop spatial links are desirable since they can transport more weights. Multi-Loop spatial links have more joints than single-loop links. In synthesis scenarios with several points or locations, they are preferred. Here three operating conditions

for a multi-loop spatial connection used to calculate the cylinder's displacement and angle (RS and SS Dyads). And Angular Position 1, and 3 for Cylinder 1, 2, and 3 correspondingly. Table 1 shows the total time needed to inflate a cylinder based on length.

MATLAB was utilized to solve all nonlinear equations obtained by thesis synthesis. Changing the program's convergence tolerance refines the result. Here exponential rotation matrix formulae apply. The loop closure equations and motion generation synthesis can synthesis all spatial linkages with reduced kinematic pairings. When generic motion equations are expressed systematically, they may be implemented in computers. Using the algebra of exponential rotation matrices, the thesis loop closure equations were reduced. These properties make dealing with matrix problems simpler.

For the purpose of reducing matrix equations arising in kinematic analysis and synthesis, the algebra of Jacobian matrices is a powerful and beautiful mathematical tool. There is little research on its use for analysing or synthesising spatial processes, although it has been used to the study of robot manipulators. Other mechanism designers may be enticed to adopt this algebra if it proves useful in solving further challenges of spatial mechanism analysis and synthesis as shown in Figures 10-12.

**Table 1.** Extendable-rod position vs. angle $\theta_1$, $\theta_2$ and $\theta_3$ position for Only One Cylinder X1

| Observation | Extendable-Rod Position in mm | | | $\theta_1$ Position for 1 | $\theta_2$ Position for 2 | $\theta_3$ Position for 3 | Tracker Mounting Plate Movement Angle |
|---|---|---|---|---|---|---|---|
| | C1 | C2 | C3 | | | | |
| 1 | 0 | NOT EXTEND | NOT EXTEND | 20 | 63 | 37 | 119 |
| 2 | 25 | NOT EXTEND | NOT EXTEND | 19.8 | 66.5 | 35.3 | 120 |
| 3 | 50 | NOT EXTEND | NOT EXTEND | 22.5 | 67.3 | 34.8 | 126.5 |
| 4 | 75 | NOT EXTEND | NOT EXTEND | 25 | 68.4 | 33.9 | 133.5 |
| 5 | 100 | NOT EXTEND | NOT EXTEND | 29.3 | 69.1 | 33.9 | 144.6 |
| 6 | 125 | NOT EXTEND | NOT EXTEND | 34.8 | 69.4 | 34.1 | 154.3 |
| 7 | 150 | NOT EXTEND | NOT EXTEND | 40 | 69.2 | 34.1 | 167 |
| 8 | 175 | NOT EXTEND | NOT EXTEND | 48.5 | 69.1 | 33.9 | 177.6 |
| 9 | 200 | NOT EXTEND | NOT EXTEND | 57.1 | 69.7 | 35.1 | 196.6 |
| 10 | 225 | NOT EXTEND | NOT EXTEND | 63.5 | 65.7 | 39.7 | 208.3 |
| 11 | 250 | NOT EXTEND | NOT EXTEND | 68.4 | 67.9 | 57.4 | 216.4 |

## 6. RESULTS AND DISCUSSION

The effectiveness of the proposed method and the RSSR-SS manipulator's dynamic equations are shown by the simulation results, as is the effect of the inertia of the Leg/ Actuator and its components on the manipulator's dynamics. Table 2 to Table 8 show the various values of the experiments.

**Table 2.** Cylinder extension position vs. angle $\theta_1$, $\theta_2$ and $\theta_3$ position for Only One Cylinder X2

| Observation | Extendable-Rod Position in mm | | | $\theta_1$ Position for 1 | $\theta_2$ Position for 2 | $\theta_3$ Position for 3 | Tracker Mounting Plate Movement Angle |
|---|---|---|---|---|---|---|---|
| | C1 | C2 | C3 | | | | |
| 1 | NOT EXTEND | 0 | NOT EXTEND | 14.9 | 65.2 | 37.8 | 125 |
| 2 | NOT EXTEND | 25 | NOT EXTEND | 18.2 | 69.2 | 39.8 | 121.8 |
| 3 | NOT EXTEND | 50 | NOT EXTEND | 22.2 | 71.3 | 43.1 | 125.7 |
| 4 | NOT EXTEND | 75 | NOT EXTEND | 27 | 72.4 | 46.6 | 131.8 |
| 5 | NOT EXTEND | 100 | NOT EXTEND | 32.1 | 75.1 | 51.6 | 144.7 |
| 6 | NOT EXTEND | 125 | NOT EXTEND | 40 | 77.1 | 55.6 | 149 |
| 7 | NOT EXTEND | 150 | NOT EXTEND | 43 | 78.5 | 59.2 | 134 |
| 8 | NOT EXTEND | 175 | NOT EXTEND | 47.6 | 80.6 | 63.3 | 128.5 |
| 9 | NOT EXTEND | 200 | NOT EXTEND | 50.6 | 83.3 | 65.7 | 130.3 |
| 10 | NOT EXTEND | 225 | NOT EXTEND | 52.8 | 86.3 | 69.7 | 124.2 |
| 11 | NOT EXTEND | 250 | NOT EXTEND | 56.2 | 88.6 | 71.5 | 116.7 |

**Table 3.** Cylinder extension position vs. angle $\theta_1$, $\theta_2$ and $\theta_3$ position for Only One Cylinder X3

| Observation | Extendable-Rod Position in mm | | | $\theta_1$ Position for 1 | $\theta_2$ Position for 2 | $\theta_3$ Position for 3 | Tracker Mounting Plate Movement Angle |
|---|---|---|---|---|---|---|---|
| | C1 | C2 | C3 | | | | |
| 1 | NOT EXTEND | NOT EXTEND | 0 | 18.4 | 64.7 | 38.5 | 120.7 |
| 2 | NOT EXTEND | NOT EXTEND | 25 | 15.8 | 63.1 | 37.4 | 116.3 |
| 3 | NOT EXTEND | NOT EXTEND | 50 | 14.5 | 61.8 | 36 | 113.7 |
| 4 | NOT EXTEND | NOT EXTEND | 75 | 13.6 | 61.4 | 35.5 | 111.1 |
| 5 | NOT EXTEND | NOT EXTEND | 100 | 13.6 | 60.9 | 34.6 | 112.3 |
| 6 | NOT EXTEND | NOT EXTEND | 125 | 14 | 60.4 | 34.6 | 116.5 |
| 7 | NOT EXTEND | NOT EXTEND | 150 | 14.4 | 60.6 | 34.6 | 119 |
| 8 | NOT EXTEND | NOT EXTEND | 175 | 15 | 60.4 | 34.3 | 121.5 |
| 9 | NOT EXTEND | NOT EXTEND | 200 | 15.6 | 60.7 | 34.6 | 111.4 |
| 10 | NOT EXTEND | NOT EXTEND | 225 | 15.6 | 61 | 34.5 | 119.5 |
| 11 | NOT EXTEND | NOT EXTEND | 250 | 16.2 | 60.4 | 34.5 | 125 |

**Table 4.** Cylinder extension position vs. angle $\theta_1$, $\theta_2$ and $\theta_3$ position for Only One Cylinder X1 and X2

| Observation | Extendable-Rod Position in mm | | | $\theta_1$ Position for 1 | $\theta_2$ Position for 2 | $\theta_3$ Position for 3 | Tracker Mounting Plate Movement Angle |
|---|---|---|---|---|---|---|---|
| | C1 | C2 | C3 | | | | |
| 1 | 0 | 0 | NOT EXTEND | 14 | 65 | 34.5 | 103 |
| 2 | 25 | 25 | NOT EXTEND | 16.7 | 69.4 | 34.9 | 113.5 |
| 3 | 50 | 50 | NOT EXTEND | 21.2 | 70.5 | 35.2 | 112 |
| 4 | 75 | 75 | NOT EXTEND | 23.9 | 75 | 35.4 | 109.4 |
| 5 | 100 | 100 | NOT EXTEND | 26.8 | 79.3 | 35.9 | 108.6 |
| 6 | 125 | 125 | NOT EXTEND | 30.7 | 83.1 | 36.5 | 115.2 |
| 7 | 150 | 150 | NOT EXTEND | 35.2 | 85.9 | 39.3 | 111 |
| 8 | 175 | 175 | NOT EXTEND | 38.5 | 89.3 | 40.4 | 113.1 |
| 9 | 200 | 200 | NOT EXTEND | 43.2 | 96.3 | 40.2 | 110.1 |
| 10 | 225 | 225 | NOT EXTEND | 48.4 | 100.1 | 43 | 108.4 |
| 11 | 250 | 250 | NOT EXTEND | 52.7 | 103.3 | 44.7 | 106.3 |

**Table 5.** Cylinder extension position vs. angle $\theta_1$, $\theta_2$ and $\theta_3$ position for Only One Cylinder X2 and X3

| Observation | Extendable-Rod Position in mm | | | $\theta_1$ Position for 1 | $\theta_2$ Position for 2 | $\theta_3$ Position for 3 | Tracker Mounting Plate Movement Angle |
|---|---|---|---|---|---|---|---|
| | C1 | C2 | C3 | | | | |
| 1 | NOT EXTEND | 0 | 0 | 14.4 | 65 | 33.6 | 105.2 |
| 2 | NOT EXTEND | 25 | 25 | 14.9 | 64.6 | 36.8 | 116 |
| 3 | NOT EXTEND | 50 | 50 | 18.2 | 65.5 | 38.3 | 107.3 |
| 4 | NOT EXTEND | 75 | 75 | 21.1 | 66.4 | 40.3 | 102.1 |
| 5 | NOT EXTEND | 100 | 100 | 32.7 | 68.1 | 41.3 | 92.5 |
| 6 | NOT EXTEND | 125 | 125 | 27.7 | 68.1 | 44.7 | 90.8 |
| 7 | NOT EXTEND | 150 | 150 | 31.8 | 68.4 | 48.1 | 93.3 |
| 8 | NOT EXTEND | 175 | 175 | 35.2 | 70.4 | 50.7 | 96.1 |
| 9 | NOT EXTEND | 200 | 200 | 38.4 | 71.3 | 54.6 | 99.4 |
| 10 | NOT EXTEND | 225 | 225 | 43.2 | 73 | 59.3 | 104.2 |
| 11 | NOT EXTEND | 250 | 250 | 49.9 | 75.3 | 65.2 | 108.7 |

**Table 6.** Cylinder extension position vs. angle $\theta_1$, $\theta_2$ and $\theta_3$ position for Only One Cylinder X1 and X3

| Observation | Extendable-Rod Position in mm | | | $\theta_1$ Position for 1 | $\theta_2$ Position for 2 | $\theta_3$ Position for 3 | Tracker Mounting Plate Movement Angle |
|---|---|---|---|---|---|---|---|
| | C1 | C2 | C3 | | | | |
| 1 | 0 | NOT EXTEND | 0 | 14.2 | 64.6 | 34.3 | 101.2 |
| 2 | 25 | NOT EXTEND | 25 | 16.6 | 63.3 | 34.3 | 116.9 |
| 3 | 50 | NOT EXTEND | 50 | 18.4 | 61.5 | 34.4 | 126.1 |
| 4 | 75 | NOT EXTEND | 75 | 20.1 | 60.9 | 34.1 | 133 |
| 5 | 100 | NOT EXTEND | 100 | 21.3 | 60.2 | 34.2 | 138.8 |
| 6 | 125 | NOT EXTEND | 125 | 22.6 | 60.5 | 34.1 | 143.1 |
| 7 | 150 | NOT EXTEND | 150 | 23.8 | 60.2 | 33.9 | 147.8 |
| 8 | 175 | NOT EXTEND | 175 | 24.8 | 59.8 | 33.9 | 151.2 |
| 9 | 200 | NOT EXTEND | 200 | 25.7 | 60.4 | 34.2 | 155.7 |
| 10 | 225 | NOT EXTEND | 225 | 26.4 | 59.8 | 34.1 | 158.2 |
| 11 | 250 | NOT EXTEND | 250 | 27.3 | 60.3 | 33.9 | 161.3 |

**Table 7.** Cylinder extension position vs. angle $\theta_1$, $\theta_2$ and $\theta_3$ position for Only One Cylinder X1, X2 and X3

| Observation | Extendable-Rod Position in mm | | | $\theta_1$ Position for 1 | $\theta_2$ Position for 2 | $\theta_3$ Position for 3 | Tracker Mounting Plate Movement Angle |
|---|---|---|---|---|---|---|---|
| | C1 | C2 | C3 | | | | |
| 1 | 0 | 0 | 0 | 13.6 | 63.6 | 34.1 | 101.4 |
| 2 | 25 | 25 | 25 | 16.6 | 65.7 | 34.6 | 105.1 |
| 3 | 50 | 50 | 50 | 19.4 | 69.1 | 34.4 | 105.4 |
| 4 | 75 | 75 | 75 | 21.7 | 70.7 | 34.5 | 109.4 |
| 5 | 100 | 100 | 100 | 24.2 | 70.3 | 34.8 | 111 |
| 6 | 125 | 125 | 125 | 26.2 | 71.8 | 35.4 | 113.3 |
| 7 | 150 | 150 | 150 | 28.1 | 73.2 | 35.7 | 119.3 |
| 8 | 175 | 175 | 175 | 30 | 73 | 36.5 | 117.1 |
| 9 | 200 | 200 | 200 | 31.9 | 73.6 | 38.8 | 120.8 |
| 10 | 225 | 225 | 225 | 33.5 | 73.9 | 39.1 | 121.3 |
| 11 | 250 | 250 | 250 | 34.7 | 74.2 | 39.9 | 124.1 |

**Table 8.** Cylinder extension time

| Stroke Length | No. of Cylinder | Rise Time (Second) | Return Time (Second) |
|---|---|---|---|
| 250 | X1 | 55.57 | 56.87 |
| 250 | X2 | 56.76 | 55.51 |
| 250 | X3 | 56.96 | 57.08 |

### 6.1 Cylinder X1 and X2 extend

Encoder variation ranges from 4° to 9.6° during combined extension of cylinder 1 and 2. Platform table remains stable at 8°-22° in X direction and 9°-21° in Y direction after 710 iterations as shown in Figure 13.

### 6.2 Cylinder X2 and X3 extend

During the operation of cylinder 2 and 3, encoder one more time with 3°-13° where is encoder to you the variation from 4°-18° with the stability also the table platform gives a negative value in the X direction, indicating that it is sustainable, and a value between 2° and 28° in the y direction. This is the outcome of 1045 iterations as shown in Figure 14.

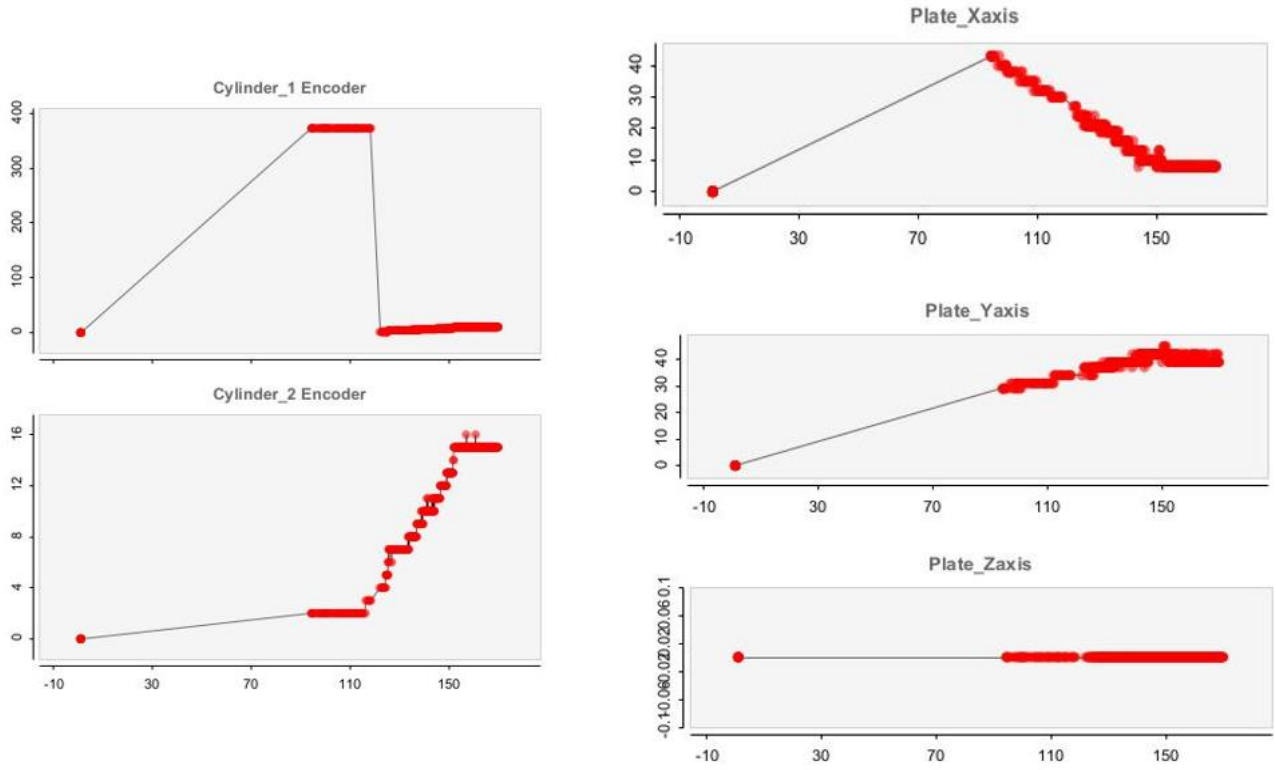


**Figure 13.** Encoder 1 and 2 and top plate position due to extending of cylinder 1 and 2

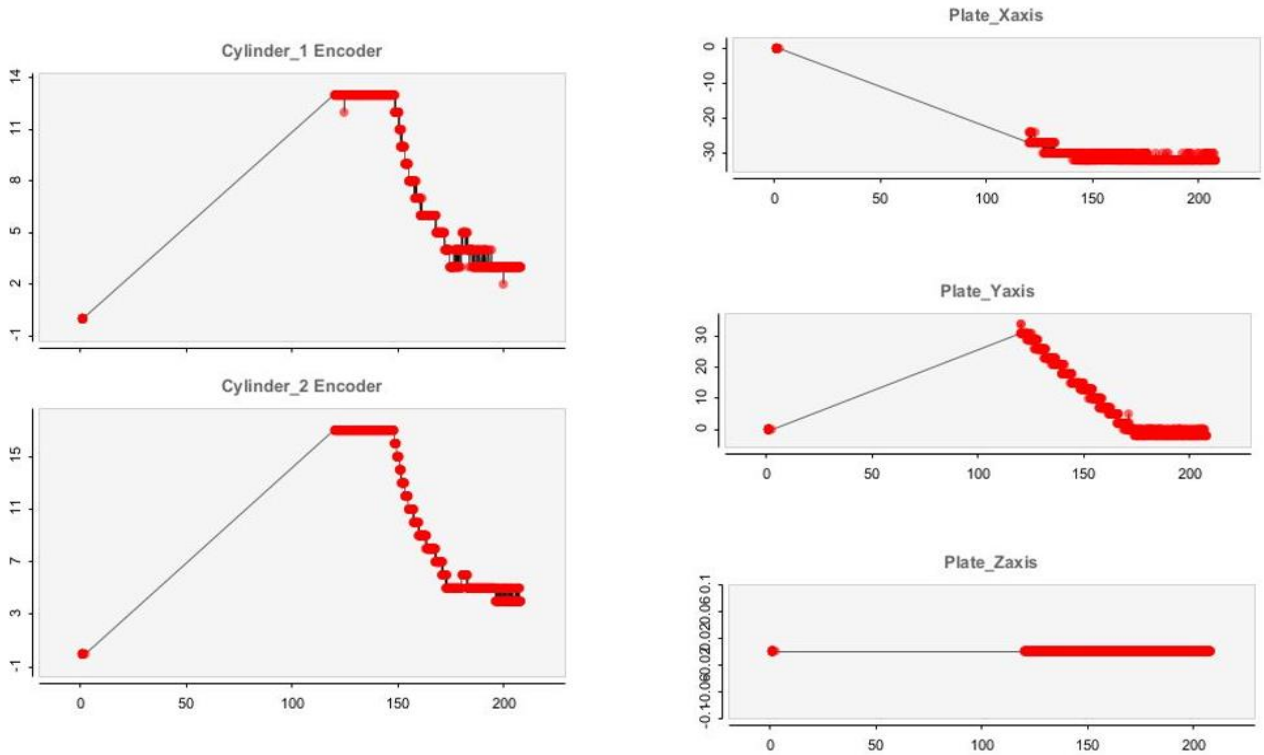


**Figure 14.** Encoder 2 and 3 and top plate position due to extending of cylinder 2 and 3

### 6.3 Cylinder X3 and X1 extend

Similarly, after 1069 readings, the graph shows combining the extension of cylinder 1 and 3 encoders from 1.2° to 29.2° and encoder to give rotation with 0° to 28° where the platform remains stable in both X and Y directions with 0°-26° as shown in Figure 15.

### 6.4 Cylinder X1, X2 and X3 extend

After combining all three cylinders in extended positions, we get stability from 1.2° to 3.6° only where When the MATLAB findings are compared to the experimental results (for the x and y axes), a maximum divergence of 3.5 percent is seen in Figure 16.

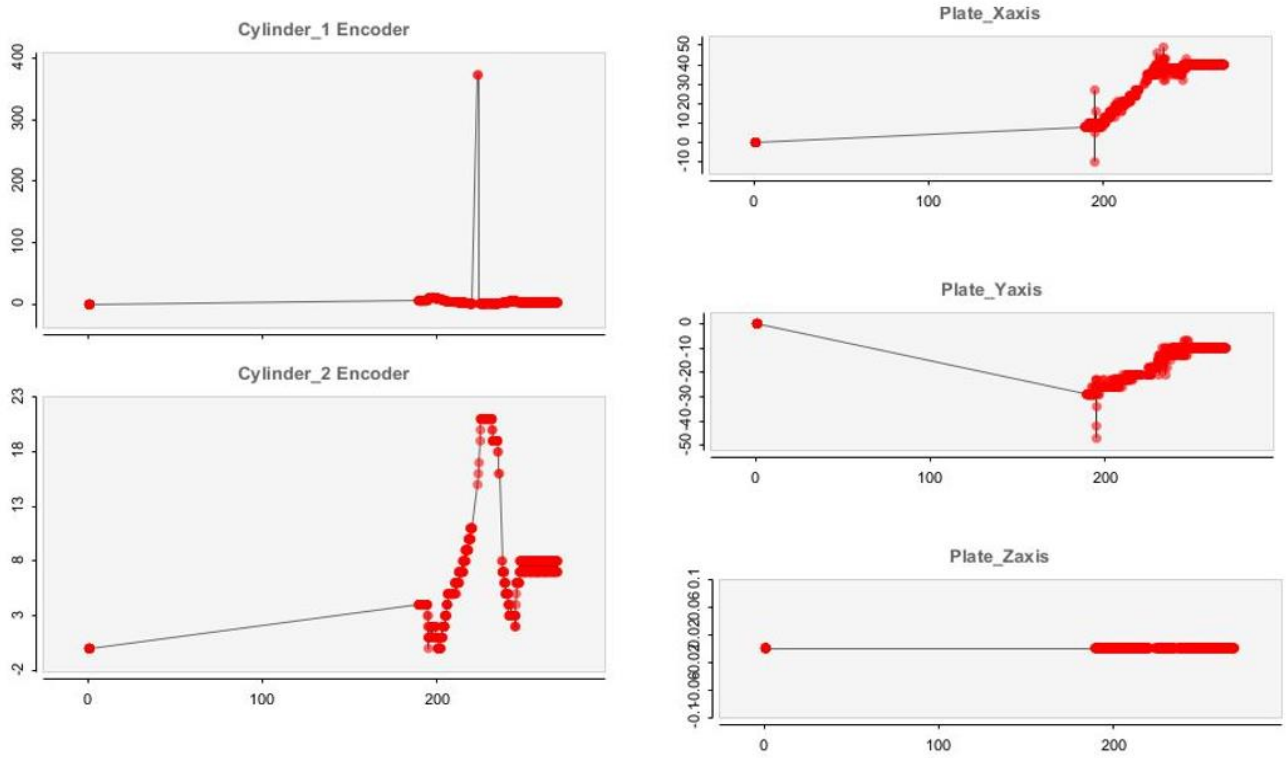


**Figure 15.** Encoder 3 and 1 and top plate position due to extending of cylinder 3 and 1

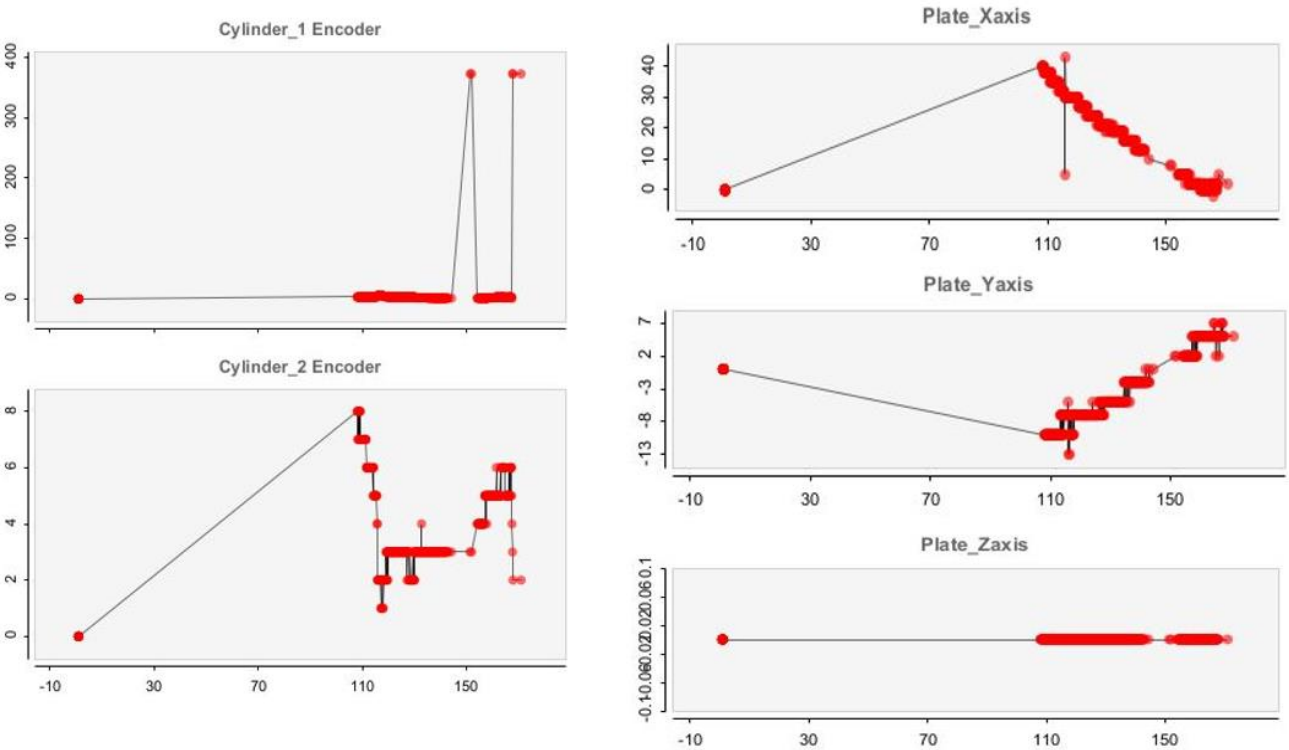


**Figure 16.** Encoder 1 and 2 and top plate position due to extending of cylinder 1, 2 and 3

## 7. CONCLUSION

From the research work, following points are concluded:

- Strong correlation between analytical, simulated, and experimental kinematic data was shown by the RSSR-SS manipulator. Therefore, verifying the closed-form Jacobian model and its dependability for motion control and positioning tasks.
- With platform tilt stability recorded over 0°–45° (x-axis) and 0°–32° (y-axis), experimental results revealed that individual actuator performance matched simulations, therefore ensuring correct movement under specified operating conditions.
- With an average of 7.5° after 735 cycles, encoder-based rotational motion stayed constant within 0°–14°, improving to 7.6° after 988 iterations. So it suggest increased long-term repeatability and motion dependability.
- When all three actuators were completely extended, preserving angular deviation within 1.2°–3.6°. It depicts the system's viability for precision-critical applications like as solar tracking or space communication, platform stability was best.
- High model integrity is shown by a tiny 3.5% difference between MATLAB simulations and actual tests. Nevertheless, limits on vibration dampening imply the necessity of further research in dynamic rigidity and stability augmentation by means of vibration analysis.

**Future work:**

- Integrate vibration dampening systems to enhance the positioning accuracy of the manipulator and reduce structural oscillation-induced performance loss.
- Create adaptive control systems for joint friction and external disturbance real-time adjustment during long running cycles.
- Integrating wireless telemetry and autonomous feedback loops will help the system to have more distant tracking and control in space conditions.

## REFERENCES


[1] Dinakaran, V.P., Balasubramaniyan, M.P., Muthusamy, S., Panchal, H. (2023). Performa of SCARA based intelligent 3 axis robotic soft gripper for enhanced material handling. Advances in Engineering Software, 176: 103366. https://doi.org/10.1016/j.advengsoft.2022.103366

[2] Dinakaran, V.P., Balasubramaniyan, M.P., Le, Q.H., Alrubaie, A.J., Al-khaykan, A., Muthusamy, S., Panchal, H., Jaber, M.M., Dixit, A.K., Prakash, C. (2023). A novel multi objective constraints based industrial gripper design with optimized stiffness for object grasping. Robotics and Autonomous Systems, 160: 104303. https://doi.org/10.1016/j.robot.2022.104303

[3] Liu, J., Yap, H.J., Mohd Khairuddin, A.S. (2024). Review on motion planning of robotic manipulator in dynamic environments. Journal of Sensors, 2024(1): 5969512. https://doi.org/10.1155/2024/5969512

[4] Mäkinen, P., Mustalahti, P., Kivelä, T., Mattila, J. (2025). Increasing the task flexibility of heavy-duty manipulators using visual 6D pose estimation of objects. arXiv Preprint arXiv:2502.19169. https://arxiv.org/abs/2502.19169

[5] Ponimatkin, G., Cífka, M., Souček, T., Fourmy, M., Labbé, Y., Petrik, V., Sivic, J. (2025). 6D object pose tracking in internet videos for robotic manipulation. arXiv Preprint arXiv:2503.10307. https://arxiv.org/abs/2503.10307

[6] Sukri, H., Ibadillah, A.F., Thinakaran, R., Umam, F., Dafid, A., Kurniawan, A., Morshed, M.M., Kurniawan, D. (2025). Enhanced precision control of a 4-DOF robotic arm using numerical code recognition for automated object handling. Journal of Robotics and Control, 6(1): 315-335. https://doi.org/10.18196/jrc.v6i1.24349

[7] Singh, N., Tewari, V.K., Biswas, P.K., Dhruw, L.K., Ranjan, R., Ranjan, A. (2024). Optimizing cotton-picking robotic manipulator and inverse kinematics modeling using evolutionary algorithm-assisted artificial neural network. Journal of Field Robotics, 41(7): 2322-2342. https://doi.org/10.1002/rob.22247

[8] Lenarčič, L., Wenger, P. (2008). Advances in Robot Kinematics: Analysis and Design. Dordrecht: Springer.

[9] Vaccaro, S., Mosig, J.R., de Maagt, P. (2003). Two advanced solar antenna" SOLANT" designs for satellite and terrestrial communications. IEEE Transactions on Antennas and Propagation, 51(8): 2028-2034. https://doi.org/10.1109/TAP.2003.815424

[10] Gholipour, R., Fateh, M.M. (2019). Designing a robust control scheme for robotic systems with an adaptive observer. International Journal of Engineering, Transactions B: Applications, 32(2): 284-291.

[11] Perez-Gracia, A. (2008). Synthesis of spatial RPRP loops for a given screw system. In New Trends in Mechanism Science, Analysis and Design, pp. 11-19.

[12] Jazar, R.N. (2010) Theory of Applied Robotics: Kinematics, Dynamics, and Control. New York: Springer.

[13] Du, X., Li, Y., Wang, P., Ma, Z., Li, D., Wu, C. (2021). Design and optimization of solar tracker with U-PRU-PUS parallel mechanism. Mechanism and Machine Theory, 155: 104107. https://doi.org/10.1016/j.mechmachtheory.2020.104107

[14] Kumar, V., Schmiedeler, J., Sreenivasan, S.V., Su, H.J. (Eds.). (2013). Advances in Mechanisms, Robotics and Design Education and Research. Springer International Publishing. https://doi.org/10.1007/978-3-319-00398-6

[15] Hubach, J.O. (2019). Solar Tracking Using a Parallel Manipulator Mechanism to Achieve Two-Axis Position Tracking. Rose Hulman Institute of Technology.

[16] Zhang, H., Fang, H., Zou, Q., Zhang, D. (2020). Dynamic modeling and adaptive robust synchronous control of parallel robotic manipulator for industrial application. Complexity, 2020(1): 5640246. https://doi.org/10.1155/2020/5640246

[17] Moore, B., Schicho, J., Gosselin, C.M. (2010). Dynamic balancing of spherical 4R linkages. Journal of Mechanisms and Robotics, 2(2): 021002. https://doi.org/10.1115/1.4001090

[18] Rezaei, A., Akbarzadeh, A., Akbarzadeh-T, M.R. (2012). An investigation on stiffness of a 3-PSP spatial parallel mechanism with flexible moving platform using invariant form. Mechanism and Machine Theory, 51: 195-216.

https://doi.org/10.1016/j.mechmachtheory.2011.11.011
[19] Bapna, D., Rollins, E., Foessel, A., Whittaker, R. (1998). Antenna pointing for high bandwidth communications from mobile robots. In Proceedings. 1998 IEEE International Conference on Robotics and Automation (Cat. No. 98CH36146), Leuven, Belgium, pp. 3468-3473. https://doi.org/10.1109/ROBOT.1998.680974
[20] Zhao, Y., Cao, Y., Kong, X., Zhao, T. (2018). Type synthesis of parallel mechanisms with a constant Jacobian matrix. Journal of Mechanisms and Robotics, 10(6): 061011. https://doi.org/10.1115/1.4040962
[21] Li, X., Ding, X., Chirikjian, G.S. (2017). Analysis of a mechanism with redundant drive for antenna pointing. Proceedings of the Institution of Mechanical Engineers, Part G: Journal of Aerospace Engineering, 231(2): 229-239. https://doi.org/10.1177/0954410016636157
[22] Li, T., Wang, Y. (2009). Deployment dynamic analysis of deployable antennas considering thermal effect. Aerospace Science and Technology, 13(4-5): 210-215. https://doi.org/10.1016/j.ast.2009.04.005
[23] Westphal, R., Winkelbach, S., Gösling, T., Oszwald, M., Hüfner, T., Krettek, C., Wahl, F.M. (2009). Automated Robot Assisted Fracture Reduction. In: Kröger, T., Wahl, F.M. (eds) Advances in Robotics Research. Springer, Berlin, Heidelberg. https://doi.org/10.1007/978-3-642-01213-6_23
[24] Bacaro, M., Cianetti, F., Alvino, A. (2014). Device for measuring the inertia properties of space payloads. Mechanism and Machine Theory, 74: 134-153. https://doi.org/10.1016/j.mechmachtheory.2013.12.008
[25] Zeng, Q., Ehmann, K.F. (2014). Design of parallel hybrid-loop manipulators with kinematotropic property and deployability. Mechanism and Machine Theory, 71: 1-26. https://doi.org/10.1016/j.mechmachtheory.2013.08.017
[26] Sokolov, A., Xirouchakis, P. (2007). Dynamics analysis of a 3-DOF parallel manipulator with R–P–S joint structure. Mechanism and Machine Theory, 42(5): 541-557. https://doi.org/10.1016/j.mechmachtheory.2006.05.004
[27] van der Wijk, V., Herder, J.L., Demeulenaere, B. (2009). Comparison of various dynamic balancing principles regarding additional mass and additional inertia. Journal of Mechanisms and Robotics, 1(4): 041006. https://doi.org/10.1115/1.3211022
[28] Patel, K., Bhatt, P.M. (2022). Modeling and dynamic analysis of multi-loop RSSR-SS parallel manipulator. Materials Today: Proceedings, 66: 2001-2007. https://doi.org/10.1016/j.matpr.2022.05.443
[29] Patel, K., Bhatt, P.M. (2019). An application of Jacobian matrix in kinematic of multi-loop spatial mechanism. International Journal of Innovative Technology and Exploring Engineering, 8(12S): 701-704. https://doi.org/10.35940/ijitee.L1166.10812S19
[30] Rao, N.M., Rao, K.M. (2009). Dimensional synthesis of a spatial 3-RPS parallel manipulator for a prescribed range of motion of spherical joints. Mechanism and Machine Theory, 44(2): 477-486. https://doi.org/10.1016/j.mechmachtheory.2008.03.001